An Automated Tool for the Detection of Electrocardiographic Diagnostic Features based on Spatial Aggregation and Computational Geometry

Liliana Ironi and Stefania Tentoni

IMATI - CNR, via Ferrata 1, 27100 Pavia, Italy

Abstract. In this work we focus on Electrocardiographic diagnosis based on epicardial activation fields. The identification, within an activation map, of specific patterns that are known to characterize classes of pathologies provides an important support to the diagnosis of rhythm disturbances that can be missed by routine low resolution ECGs. Through an approach grounded on the integration of a Spatial Aggregation (SA) method with concepts borrowed from Computational Geometry, we propose a computational framework to automatically extract, from input epicardial activation data, a few basic features that characterize the wavefront propagation, as well as a more specific set of diagnostic features that identify an important class of rhythm pathologies due to block of conduction.

1 Introduction

One of the most important application domains where imaging has proved extremely useful is Medical Diagnosis. The process of identifying a pathological condition can be greatly supported by signs of deviations from normality that can be drawn from images. Within this context the term “imaging” usually refers to techniques to build images of anatomical districts of the human body (e.g. radiographies, CAT, NMR); more broadly, it can include methods that provide graphical representations of spatially referenced variables related to specific organ functions (e.g. EEG, ECG signals, activation maps), and in this case the term “functional” imaging is more appropriate.

Many functional images are graphical representations of a physical field: a potential contour map, for instance, is the spatial representation of a potential field. Thereby, the task of analyzing such images is not adequately tackled by traditional Image Processing methods, which have been designed for raster images. The issue of unveiling the salient physical events underlying a functional image is more appropriately and effectively addressed through feature extraction methods that can exploit the domain-specific knowledge at different abstraction levels. Such an issue is particularly relevant in view of performing explanation and automated reasoning tasks.

Within the field of Qualitative Spatial Reasoning, Spatial Aggregation (SA) [1] provides an appropriate conceptual framework for feature extraction at multiple levels, according to a powerful hierarchical abstraction strategy. In the direction of making the approach more robust and integrating, within the basic SA framework, methods

Ironi L. and Tentoni S..
An Automated Tool for the Detection of Electrocardiographic Diagnostic Features based on Spatial Aggregation and Computational Geometry.
DOI: 10.5220/0003197500030012
In *Proceedings of the 2nd International Workshop on Medical Image Analysis and Description for Diagnosis Systems* (MIAD-2011), pages 3-12
ISBN: 978-989-8425-38-6

from quantitative research fields, several works have contributed to make it an attractive framework for the development of functional imaging tools [2, 3]. Any such tool would ground on domain-specific knowledge, as the inference mechanisms rely on a network of relations that, besides dealing with spatial properties, explicitly encode such knowledge.

This work contributes to the on-going research effort aimed at delivering novel tools to support the assessment of the electric cardiac function. Diagnosing the cardiac electric function has always been a hard task for the difficulty met in the identification of salient electrical events and their spatial association with specific epicardial sites. In the clinical context, diagnosis of conduction pathologies is still carried out on the ECG signals. Several tools exist for automated ECG segmentation and classification, most of which are based on the integration of wavelet transforms with neural/fuzzy-neural networks, to deal respectively with the signal decomposition and classification tasks (see for example [5]). Within AI, Qualitative Reasoning has also played an important role in providing a number of automated ECG interpretation tools [6–8]. Unfortunately some important rhythm disturbances may be incorrectly located or missed by routine ECGs. Even body surface high resolution mapping may fail because signs of cardiac electrical events on the torso surface are weak.

In recent years, model-based numerical inverse procedures have made it possible to obtain non-invasively the epicardial activation field from body surface data. That has engaged researchers in the effort towards novel methods for electrocardiographic imaging [9, 10]. However, the interpretative rationale for cardiac maps is only partially defined, and the ability to abstract the most salient visual features from a map and relate them to the complex underlying phenomena still belongs to few experts. Due to the extreme complexity of the physical system the task of automating diagnosis of conduction disturbances from a 2D/3D activation field is therefore hard, and necessarily limited to the current interpretation rationale. Within this field functional image-based diagnosis is at its beginning, and, in accordance with the available rationale, currently regards only a few classes of conduction disturbances. The potential of Qualitative Spatial Reasoning in contributing to its development is high: a tool for the automated extraction of spatially referenced features of the cardiac electrical function would bridge the gap between established research outcomes and clinical practice.

To detect salient spatiotemporal features in the epicardial activation field, we exploit the inference mechanisms provided by a computational tool grounded on Spatial Aggregation and on Computational Geometry concepts: from a given numeric field we extract spatial objects that, at different abstraction levels, qualitatively characterize spatiotemporal phenomena, and discover and abstract patterns diagnostically relevant.We focus on epicardial activation maps, which convey information about the heart electric function in terms of the depolarization wavefront kinematics and are very useful to diagnose rhythm disturbances. We describe how to abstract, from the given activation data, such basic propagation features as the sites where the wavefront breaks through and where it terminates, or its qualitative velocity patterns, and we define a set of distinctive features that identify an important class of rhythm disturbances due to blocks of conduction.

2 Feature Abstraction from a Numeric Field

The comprehension of physical phenomena benefits from the visualization of the spatial course of relevant variables. A visual representation obtained from a given numeric field can be further inspected, and searched for homogeneities and specific patterns that have a physical meaning. This "imagistic" reasoning activity, that goes beyond mere visualization, is performed at multiple levels through a sequence of abstractions and manipulations of spatial objects that capture key physical properties.

2.1 Spatial Aggregation

Spatial Aggregation (SA) is a general-purpose framework that provides a suitable ground to capture spatiotemporal adjacencies at multiple scales in spatially distributed data. It was designed to derive and manipulate qualitative spatial representations that abstract important features of the underlying data, for their use in automated reasoning tasks [1–3]. In outline, SA transforms a numeric input field into a multi-layered symbolic description of the structure and behavior of the physical variables associated with it. This results from iterating transformations of lower-level objects into more abstract ones through the exploitation of qualitative equivalence properties shared by neighbor objects.

SA abstraction mechanisms are based on three main steps, namely *Aggregation*, *Classification*, and *Redescription*, that exploit domain-specific knowledge and spatial adjacencies (see Fig.1):

1. *Aggregation.* Spatial adjacency of low-level objects is encoded within a neighborhood graph.
2. *Classification.* Neighbor objects are grouped by similarity, according to a domain-specific equivalence predicate that defines a feature of interest.
3. *Redescription.* Similarity classes are singled out as new high-level objects that provide an abstract representation of the feature.

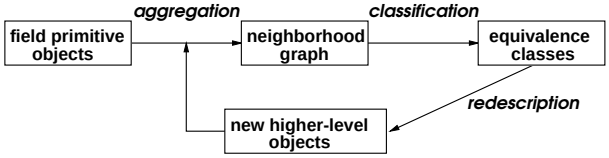

Fig. 1. Basic inference steps in Spatial Aggregation.

Step 1 mostly exploits geometrical properties, either metrical or topological. Its robustness is ensured by taking into account also the available non-geometrical knowledge, associated with the objects to be aggregated and related to the physical context [2]. Step 3 is crucial in that a non-effectual redescription of new objects may jeopardize subsequent abstractions stemming therefrom. Such steps are iterated over and over until the behavioral and structural information about the underlying physical phenomenon, required to perform a specific task, is extracted from the data set. The hierarchical structure of the whole set of the so-built objects defines a bi-directional mapping between

higher and lower-level aggregates, and, consequently, it facilitates the identification of the pieces of information relevant for a specific task.

2.2 The Role of Computational Geometry

Within the SA abstraction mechanism, *Redescription* instantiates visual features that play a role in the spatial reasoning process. The geometric representation of new objects must convey a meaningful effectual visual synthesis of the underlying similarity class. Computational Geometry methods and concepts play an important role in providing algorithms for the redescription of newly abstracted objects.

An important class of objects whose representation particularly needs to suit the reasoning task is that of 2D bounded regions. These latter can result, for example, from the application of a similarity relation grounded on interval values to a set of contiguous isopoints. The similarity classes correspond to regions that need to be instantiated as new geometrical objects for further treatment. In many situations the qualitative topological structure of the region needs to be captured at multiple scales.

The choice of the most appropriate format and scale for the redescribed object is always task-driven. For qualitative reasoning tasks, a region descriptor should be:

i) robust and stable with respect to noise and small perturbations of the region boundary,
ii) capable to roughly capture the location and global extent of the region,
iii) capable to capture the topological structure of the region at an appropriate scale of details with respect to the task, and of course
iv) computationally feasible.

An effectual representation of a region can be provided by its "gross skeleton", as defined in the following. The concept of gross skeleton is derived from the "medial axis", which is geometrically defined as the locus of the centers of circles that are internally tangent to the region's boundary. The medial axis is a sort of geometric skeleton of the figure, and its complexity, given by the number of branches, corresponds to the boundary complexity, defined as the number of its curvature extrema. Unfortunately, that makes it very sensitive to small perturbations of the boundary: noisy contours produce many secondary branches. For its instability the medial axis is not suitable as a figure descriptor in contexts affected by noise, and as such it is also inappropriate where finer scale details are irrelevant and need to be ignored.

Exact computation of the medial axis is difficult in general. An approximation of the medial axis of a region can be obtained from the Voronoi diagram related to a finite set of points that sample the region's boundary [11]. The following algorithm builds a robust simplified topological skeleton of a given polygonal region, namely the gross skeleton, by exploiting a relevance measure [12] to selectively prune the approximated Voronoi medial axis.

Algorithm (*gross skeleton construction)***.**

Given $\{P_1, ..P_n\}$, vertices of a polygonal region $\mathcal{L}$, and a threshold $\beta^* \in (0, 1)$,

1. Compute $\mathcal{M}$, Voronoi approximation of the medial axis of $\mathcal{L}$, as follows:

(a) Build the Voronoi diagram related to the set of vertices $\{P_1, ..P_n\}$,
(b) Retain only the edges that are completely internal to $\mathcal{L}$.

2. Compute the "index of relevance" $\beta(E)$ of each edge $E \in \mathcal{M}$, as

$$\beta : \mathcal{M} \rightarrow (0,1) \qquad \beta(E) = 2|l|/|\partial\mathcal{L}|$$

where if P_i, P_k are the generators of Voronoi edge E, $|l|$ is the length of shortest polygonal path connecting P_i with P_k along the region's boundary $\partial\mathcal{L}$, and $|\partial\mathcal{L}|$ is the regions's perimeter (Fig.2).

3. (*Selective pruning*) Initialize $\mathcal{L}^* := \mathcal{M}$, and $\forall E \in \mathcal{M}$ do

$$\text{if } \beta(E) < \beta^* \text{ then } \mathcal{L}^* := \mathcal{L}^* \backslash \{E\}.$$

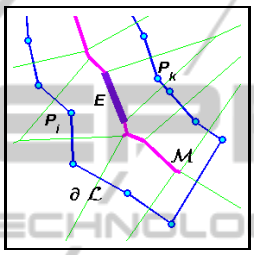

Fig. 2. Steps in the construction of the gross skeleton of a polygonal region. Vertices P_i, P_k of the region's boundary generate Voronoi edge E (thicker line). Part of the Voronoi tessellation (thin lines), and of the approximated medial axis $\mathcal{M}$ (thick line) are also shown.

Selective pruning of the medial axis $\mathcal{M}$ is performed according to an edge relevance criterion by which irrelevant boundary details are dropped: edges with a very low β value have a negligible effect on the region's boundary. The result is a connected linear structure that reflects the global topological structure of the region, as well as its rough location and spatial extent. The choice of the relevance threshold β^* affects the complexity of the resulting gross skeleton $\mathcal{L}^*$, and adjusts the descriptor to the scale required by the reasoning task: as greater β^* is, as more simplification is required.

In Fig. 3 a few perturbations of a smooth sample region are reported: in each case both the Voronoi medial axis and the gross skeleton are computed. The figure clearly shows how more robust the gross skeleton is with respect to the Voronoi medial axis approximation, and how the global shape of the region is captured.

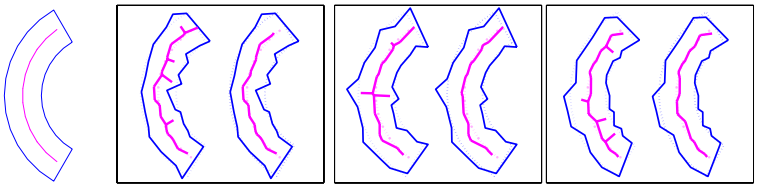

Fig. 3. A set of perturbations of the smooth region shown on the left. In each panel: the Voronoi based medial axis (left), and the gross skeleton obtained by pruning with $\beta^* = 0.25$ (right).

3 Functional Imaging of the Cardiac Electric Function

The heart is site of cyclic electrical activity which causes the muscle to rhythmically contract. The propagation of the electric excitation within the myocardium is a quite complex 4D spatiotemporal process that electrocardiologists explore on reference surfaces (epicardial, endocardial) by means of relevant variables, such as the electric potential, the activation time and the wavefront propagation velocity. Due to the difficulty of combining spatial and temporal aspects, exploring the potential $u(\mathbf{x}, t)$, a function of space and time, is a hard task. A more global and synthetic view on the spatiotemporal process of excitation is provided by the epicardial representation of the *activation time* $\tau(\mathbf{x})$, defined as the instant at which an epicardial site $\mathbf{x}$ changes its electric state from resting to activated. Such an instant is commonly estimated as the point of minimum derivative extracted from the electrogram $t \rightarrow u(\mathbf{x}, t)$. Therefore, the activation time embeds a qualitatively significant event in the electric potential time course, and, when spatially represented on the whole epicardial surface, it holds a powerful diagnostic potential.

In imaging of the cardiac electric function, an important role is played by activation maps: such maps are contour maps of the activation time that convey information about the wavefront structure and propagation. In [4], in accordance with the existing rationale of interpretation, the problem of defining and abstracting, within the SA framework, a set of spatial objects that capture a few important basic features of activation was tackled: isochrones, whose spatial sequence depicts the spread of excitation by snapshots, wavefront breakthrough and exit locations, fast propagation pathways.

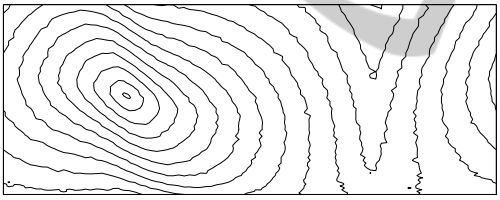

Fig. 4. Activation map as obtained from noisy data.

As an example, Fig. 4 shows an activation map obtained from noisy simulated data related to a case of normal propagation elicited by single site pacing. Let us remark that the activation time field is actually related to a 3D model of the epicardium; in order to have a unique global planar view with minimal spatial distortion, we operate on an axial cylindrical projection (Fig. 5). After preliminary noise removal, from the activation field the main wavefront propagation features are detected: the sequence of isochrones, the breakthrough and extinction sites, which respectively mark where excitation starts and ends on the epicardial surface, and the fast propagation pathways (Fig. 6).

Our work focusses on an important class of pathological conditions, namely *reentry ventricular tachycardia* (VT), and provide SA-based definitions and algorithms for the abstraction and spatial redescription of the features involved. Reentry VT is usually triggered by the presence of post-infarction scar tissue that slows conduction (propagation velocity ≤ 0.1 m/sec, [13]). When this happens, an anomalous activation pattern,

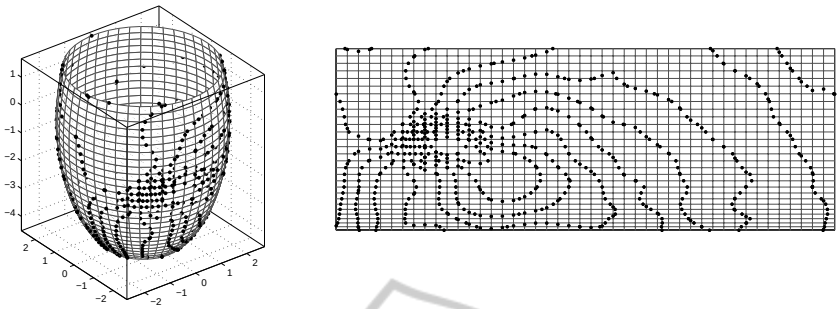

Fig. 5. Isopoints (black dots) on the epicardial surface: the surface mesh is shown. Left panel: 3D geometry. Right panel: 2D cylindrical projection.

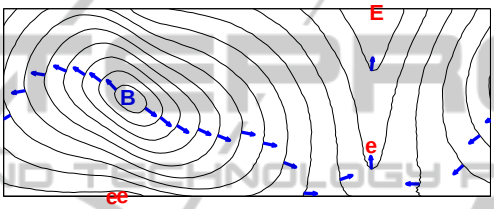

Fig. 6. Main wavefront propagation features abstracted from the sample data of Fig. 4: activation isochrones, breakthrough (B) and exit sites (e/E), and fast propagation pathways (thick vectors).

called “reentry”, can appear: the excitation wavefront travels in single/multiple circular patterns, and reenters the area where it arose from. Much research effort has been devoted to the study and characterization of this disorder. [14–16].

The key components of the reentrant VT pattern, in terms of wavefront kinematics, are (i) a *cul-de-sac*-like region (isthmus), bounded by lines of block; (ii) a breakthrough site in the isthmus area; (iii) a reentry propagation pattern; (iv) an excitation end site located proximal to the breakthrough, outside the blocked area.

Given the discretized epicardial geometry Ω_h and the activation time field $\tau = \tau(\mathbf{x_i}),\ \mathbf{x_i} \in \Omega_h$, the main steps carried out to map it to a structural spatial representation of the salient propagation features, including the possible presence of a reentry VT pattern, are here very briefly summarized:

1. Breakthrough and exit sites, isopoints, and the time sequence of the isochrones are first obtained [4];
2. The velocity field is computed as $\mathbf{v}(\mathbf{x}) = \nabla\tau(\mathbf{x})/|\nabla\tau(\mathbf{x})|^2$ where ∇ is the gradient operator [17]. By mapping the velocity module range into a small set of qualitative values, e.g. *very-slow, slow, medium, high*, in accordance with threshold values suggested by the experts, the epicardial surface gets partitioned into homogeneous subregions, each of them labeled by the qualitative value of the velocity module. In this context, the value *very-slow* marks a pathological condition. Then:
3. If the region $\mathcal{L}$, labeled *very-slow* , is not empty,

(a) it gets redescribed by its gross skeleton, $\mathcal{L}^*$, which represents the abstracted *"conduction block"* line;
(b) a set of propagation lines, obtained as stream lines of the vector field, are generated from a neighborhood of the ends of the block line, and classified into *"main propagation"* classes according to their ending site;
(c) among the ending sites associated with the main propagation paths, the nearest to the isthmus area is located (loop pattern).

Step 3 aims at discovering and abstracting a possible reentry circuit by singling out its key components. Let us remark that noisy data should be properly pre-processed to reduce noise to acceptable levels and allow reliable and robust feature extraction. Data smoothing actually corresponds to how the expert approaches the visual reasoning task, by getting rid of minor or spurious details to catch the main patterns.

Figure 7 shows, for the data set corresponding to Fig. 5, a detail of the area where isochrones are spatially denser: the boundary $\partial\mathcal{L}$ of a critical *very-slow* region is shown, as well as the Voronoi based medial axis $\mathcal{M}$, and the gross skeleton $\mathcal{L}^*$ (left panel). In the right panel, the abstracted conduction block complex: a cul-de-sac region where isochrones get more crowded, bounded by a line of block which separates a breakthrough and an extinction sites, spatially close to each other. The line of block, extracted as gross skeleton of the *very-slow* area, corresponds to merging the locally crowded isochrones.

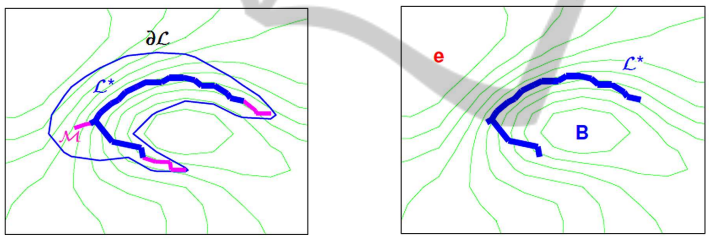

Fig. 7. Left panel: the approximated medial axis $\mathcal{M}$ (thick line), and its pruned version $\mathcal{L}^*$ (dark thick line) are shown within the very-low-velocity area bounded by $\partial\mathcal{L}$. Right panel: the conduction block, extracted as a line of block (gross skeleton of the critical velocity area) which leaves a breakthrough and an extinction site at opposite sides.

Figure 8 shows the global outcome of the abstraction processes. It consists of: the sequence of activation isochrones, the breakthrough and exit sites, the discovered block of conduction, and the reentrant propagation patterns, starting at the ends of the block arc.

4 Discussion and Conclusions

The approach herein proposed to automatically capture specific aspects of cardiac electrical activity is of broad methodological interest to electrocardiography, and more in general, to medical imaging. It results from the integration of standard computational

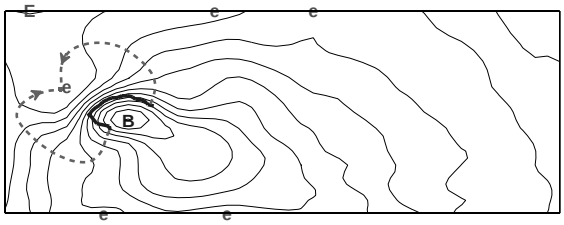

Fig. 8. Outcome of the abstraction processes: activation isochrones (thin solid lines), breakthrough/exit sites (B/E labels), and the block of conduction (thick solid line). A couple of wavefront propagation lines, starting at the ends of the block arc, are shown (dashed thick lines).

geometry concepts with a spatial aggregation methodology. This latter, that aims at interpreting a numeric input field, allows us to capture structural information about the underlying physical phenomenon, and to identify its global patterns and the causal relations between them. Thanks to its hierarchical strategy in extracting objects at different scales, it facilitates the definition of inference rules that favor automated reasoning on spatiotemporal phenomena to perform a specific task.

Tested on a few sample data sets regarding cases of both normal and abnormal propagation, the proposed methodology proved effective in the identification, from input activation data, of the salient epicardial wavefront kinematics, and of specific spatiotemporal features that characterize an important class of arrhythmias. At the current stage of development, the analysis is limited to simplified scenarios, for which an interpretative rationale is available. However, the results obtained even in presence of mild noise make us confident about the feasibility of the realization, in the long term, of an intelligent system for electrocardiac image understanding, based on such an approach. Further work will regard:

(i) the validation of the methodology on measured data, to assess its weaknesses and strengths when applied in a clinical context. To this regard, sensitivity to noise should be more deeply investigated;
(ii) the study of more complex phenomena, such as those involving the Purkinje network or multiple stimuli, and the proper characterization and identification of all propagation aspects;
(iii) the definition of a strategy for the comparison of the features of a given map against those of a *nominal* one, with the aim to detect and explain possible deviations from the expected patterns.

As for the realization of a complete diagnostic tool for cardiac electric activity, further insight into the electric function could be drawn from the analysis of temporal sequences of potential data. From these data, especially intramural measurements, we could derive information about the electrical activity prior to its surface breakthrough that is complementary with respect to that obtainable from surface activation data. That would allow us to locate intramural components of reentry pathways associated with arrhythmogenic activity. However, the challenge of combining spatial and temporal aspects in a full 4D analysis goes with the still incomplete rationale of interpretation of such maps, and makes advances in this direction more remote.

From a broader application perspective, besides contributing to a diagnostic tool specifically designed for rhythm disturbances, the methodology we propose could be used in a therapeutical context to evaluate the efficacy of a drug therapy aimed at normalizing the rhythm, through the detection of its effects on the spatial activation patterns.

References

1. Yip, K., Zhao, F.: Spatial aggregation: Theory and applications. J Artif Intell Res 5 (1996) 1–26
2. Ironi, L., Tentoni, S.: On the problem of adjacency relations in the spatial aggregation approach. In Proc. 17th Int. Workshop on Qualitative Reasoning. (2003) 111–118
3. Ironi, L., Tentoni, S.: Towards automated electrocardiac map interpretation: an intelligent contouring tool based on spatial aggregation. In Berthold, M.R., Lenz, H.J., Bradley, E., Kruse, R., Borgelt, C., eds.: Advances in Intelligent Data Analysis V, Berlin, Springer (2003) 397–417
4. Ironi, L., Tentoni, S.: Automated detection of qualitative spatio-temporal features in electrocardiac activation maps. Artif Intell Med 39 (2007) 99–111
5. Clifford, G. D., Azuaje, F., McSharry, P. E., eds.: Advanced Methods and Tools for ECG Analysis. Artech House Publishing, Boston/London (2006)
6. Bratko, I., Mozetic, I., Lavrac, N.: Kardio: A Study in Deep and Qualitative Knowledge for Expert Systems. MIT Press, Cambridge, MA (1989)
7. Weng, F., Quiniou, R., Carrault, G., Cordier, M. O.: Learning structural knowledge from the ECG. In: ISMDA-2001. Volume 2199. Berlin, Springer (2001) 288–294
8. Kundu, M., Nasipuri, M., Basu, D. K.: A knowledge based approach to ECG interpretation using fuzzy logic. IEEE T Syst Man Cyb 28 (1998) 237–243
9. Oster, H. S., Taccardi, B., Lux, R. L., Ershler, P. R., Rudy, Y.: Noninvasive electrocardiographic imaging: reconstruction of epicardial potentials, electrograms, and isochrones and localization of single and multiple electrocardiac events. Circulation (1997) 1012–1024
10. Ramanathan, C., Ghanem, R. N., Jia, P., Ryu, K., Rudy, Y.: Noninvasive electrocardiographic imaging for cardiac electrophysiology and arrythmia. Nat Med (2004) 1–7
11. Brandt, J. W., Algazi, V. R.: Continuous skeleton computation by Voronoi diagram. CVGIP: Image understanding 55 (1992) 329–338
12. Sakai, H., Sugihara, K.: A method for stable construction of medial axes in figures. Electron Comm Jpn 2 89 (2006) 48–55
13. Cranefield, P. F.: The Conduction of the Cardiac Impulse: the Slow Response and Cardiac Arrhythmias. Futura Publishing Co, Mount Kisco NY (1975)
14. Burnes, J. E., Taccardi, B., Rudy, Y.: A noninvasive imaging modality for cardiac arrhythmias. Circulation 102 (2000) 2152–2158
15. Burnes, J. E., Taccardi, B., Ershler, P. R., Rudy, Y.: Noninvasive electrocardiogram imaging of substrate and intramural ventricular tachycardia in infarcted hearts. J Am Coll Cardiol 38 (2001) 2071–2078
16. de Bakker, J. M., van Capelle, F. J., Janse, M. J., Tasseron, S., Vermeulen, J. T., de Jonge, N., Lahpor, J.R.: Slow conduction in the infarcted human heart. Zigzag course of activation. Circulation 88 (1993) 915–926
17. Colli Franzone, P., Guerri, L., Pennacchio, M.: Spreading of excitation in 3-D models of the anisotropic cardiac tissue. II. Effect of geometry and fiber architecture of the ventricular wall. Math Biosci 147 (1998) 131–171